

Supplementary Material

Conformational states control Lck switching between free and confined diffusion modes in T cells

Geva Hilzenrat^{1,2}, Elvis Pandžić³, Zhengmin Yang^{1,2}, Daniel J. Nieves^{1,2}, Jérémie Rossy⁴, Katharina Gaus^{1,2*}

¹EMBL Australia Node in Single Molecule Science, School of Medical Sciences, University of New South Wales, Sydney, Australia

²ARC Centre of Excellence in Advanced Molecular Imaging, University of New South Wales, Sydney, Australia

³BioMedical Imaging Facility, Mark Wainwright Analytical Centre, University of New South Wales, Sydney, Australia

⁴Biotechnology Institute Thurgau, University of Konstanz, Kreuzlingen, Switzerland

* Corresponding author: k.gaus@unsw.edu.au

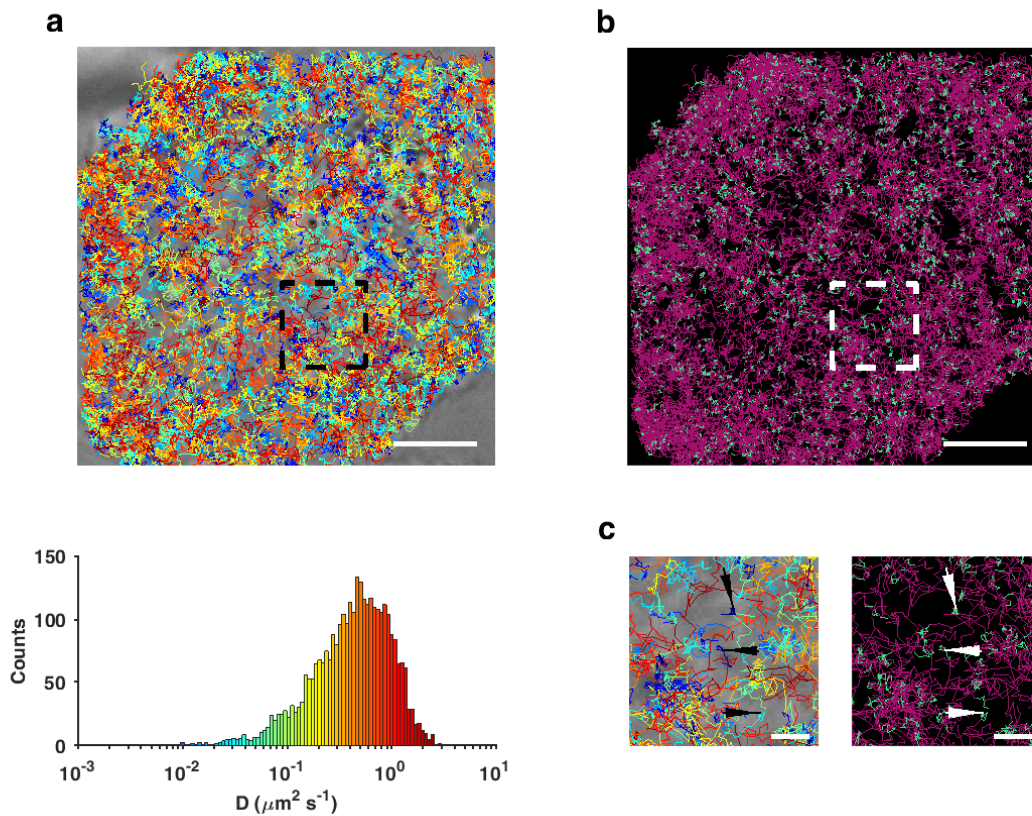


Figure S1. Diffusion and confinement relationship. **(a)** Trajectories of wtLck overlaid on a wide-field image of an activated Jurkat cell (top). Each trajectory is color-coded according to its initial diffusion coefficient (bottom), calculated by using the mean-squared displacement and the ratio $\text{MSD} = 4D\tau$ where τ is $(\text{frame rate})^{-1}$. The bottom panel also shows the distribution of diffusion coefficients for that cell. Scale bar = $5 \mu\text{m}$. **(b)** Trajectories overlaid with confined (cyan) and free (magenta) periods. Scale bar = $5 \mu\text{m}$. **(c)** $5 \mu\text{m} \times 5 \mu\text{m}$ regions of interest from (a) and (b) on the left and right, respectively. The arrows point at trajectories that initially had a small diffusion coefficient, and those consecutive events of slow diffusion were also identified as confinement events. However, particles can toggle between free and confined states, where periods of higher variance and lower variance were found to be free and confined, respectively.

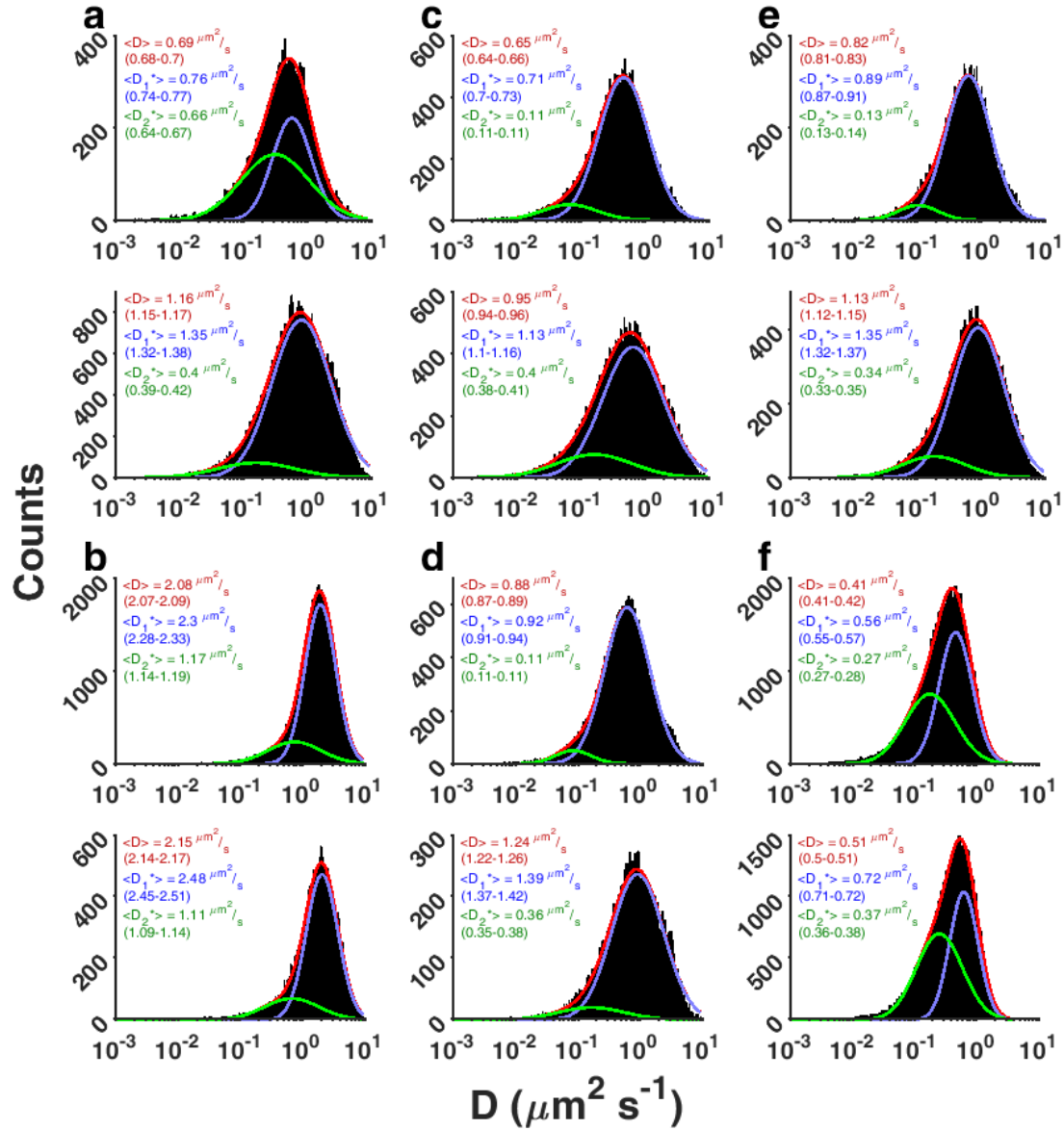


Figure S2. Diffusion coefficients histograms of (a) wtLck, (b) Lck10, (c) Lck^{Y505F}, (d) Lck^{Y394F}, (e) Lck^{K273R} and (f) Lck^{K273R, Y505F} in stimulated (top) and resting (bottom) Jurkat cells. The total average diffusion coefficient ($\langle D \rangle$) was calculated as the arithmetic mean of each total dataset, whereas $\langle D_1^* \rangle$ and $\langle D_2^* \rangle$ were derived from calculating the mean of 10,000 numbers randomly sampled for each fitted Gaussian distribution (green and blue) with the red curve showing the sum of the two distribution. The range of diffusion coefficients for each population is the 95% bootstrap confidence interval, taken by sampling each sub-population 10,000 times.

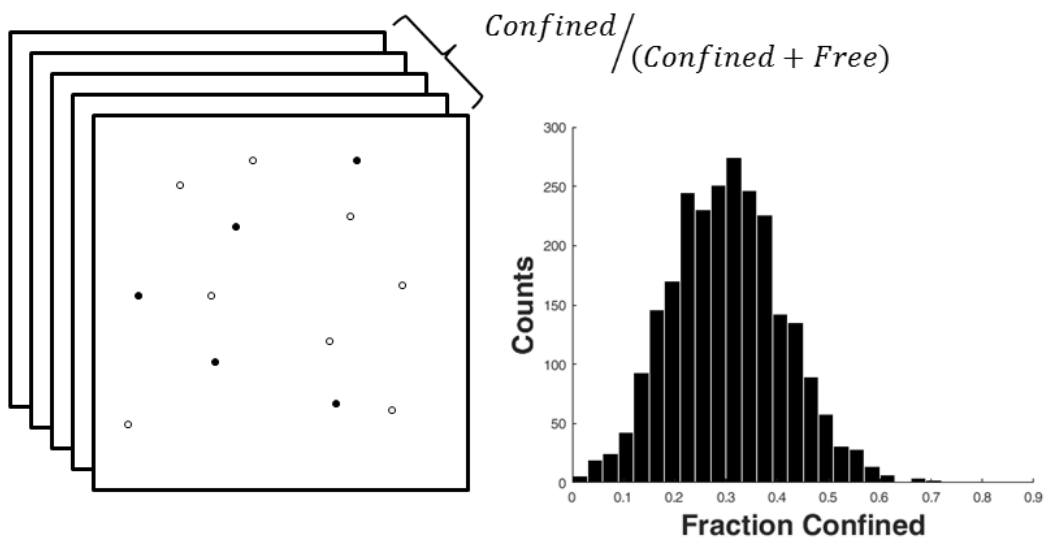


Figure S3. Illustration of confinement ratio analysis. Every sequence contains 10,000 frames. In every frame, each particle was marked as confined (black circle) or free (empty circle) according to its state as calculated via equation 1. The ratio of the sum of confined particles over the total number of particles was calculated for every 5 consecutive frames and summarized in a histogram.

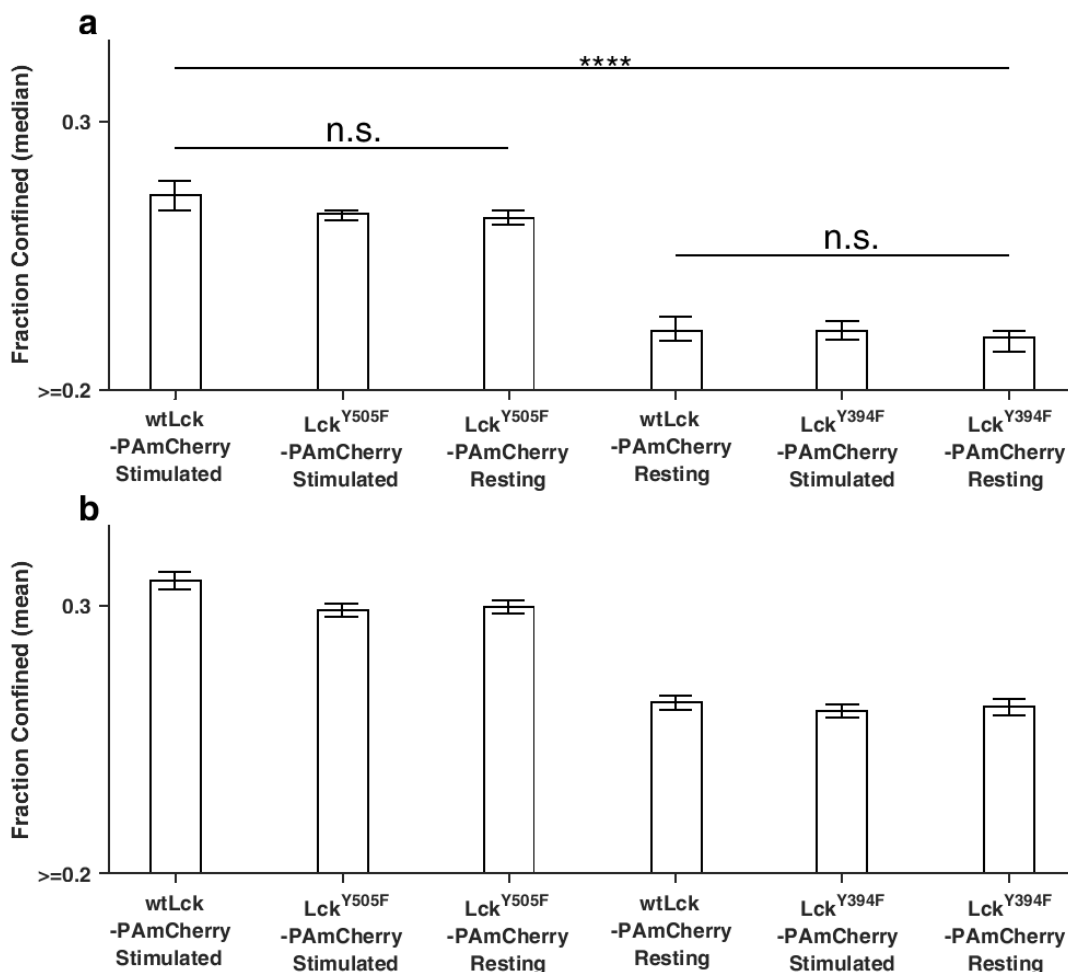


Figure S4. Comparison of confinement analysis result (a) Median values of the confined fraction for different Lck variants and the result of a Kruskal-Wellis test with a null hypothesis rejection probability threshold of $p = 0.01$. **(a)** Arithmetic mean values obtained for each condition. **(b)** Mean values of the confined fractions for each Lck variant. Error bars show the 95% bootstrap confidence interval by sampling each population 10,000 times.

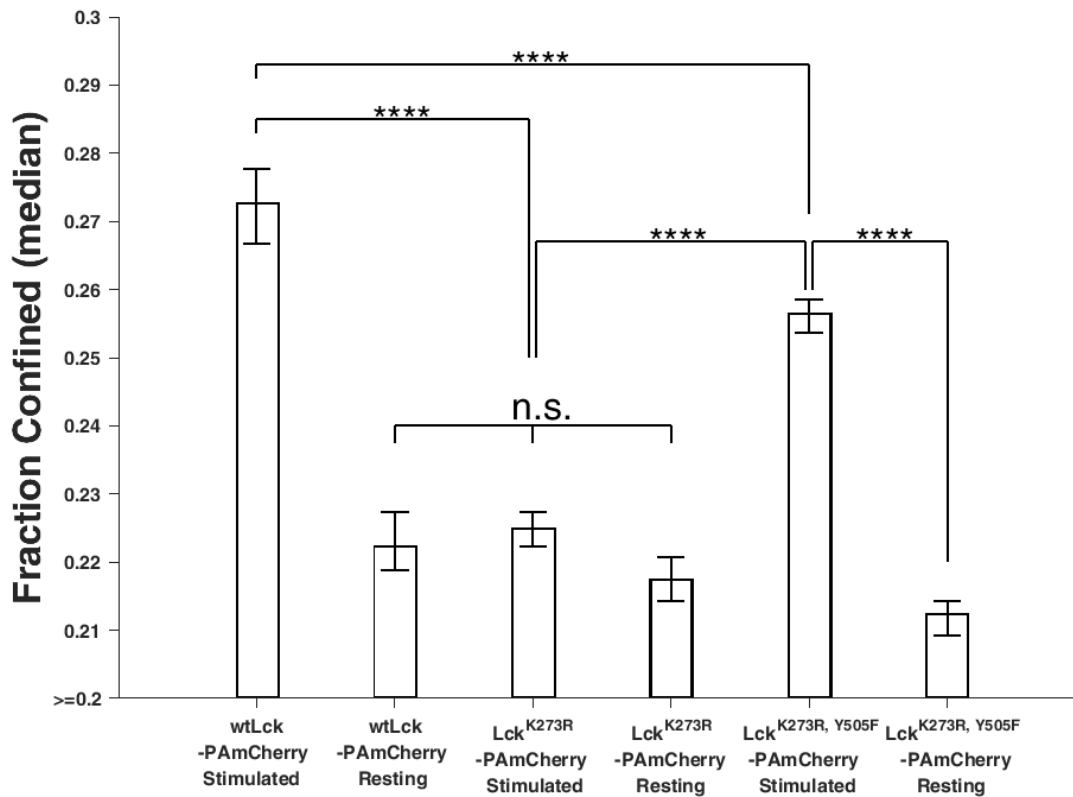


Figure S5. Comparison of confinement analysis result of wtLck-PAmCherry, Lck^{K273R}-PAmCherry and Lck^{K273R, Y505F}-PAmCherry in stimulated and resting cells. Median values of the confined fraction for different Lck variants and the result of a Kruskal-Wellis test with a null hypothesis rejection probability threshold of $p = 0.01$. Error bars show the 95% bootstrap confidence interval by sampling each population 10,000 times.